Solvent Polarity at Polar Solid Surfaces: The Role of Solvent Structure

Xiaoyi Zhang,[†] Margaret M. Cunningham,[‡] and Robert A. Walker*[,†,‡]

Chemical Physics Program and Department of Chemistry and Biochemistry, University of Maryland−College Park, College Park, Maryland 20742

Received: April 29, 2002; In Final Form: September 5, 2002

Resonance enhanced second harmonic spectra of the chromophore 4-aminobenzophenone (4ABP) were recorded at different solid/liquid interfaces. The solid substrates were hydrophilic silica and the solvents varied in size, shape and dielectric properties. Solvatochromic comparisons between SHG spectra of adsorbed 4ABP and excitation spectra of 4ABP in bulk solution reveal how solvent−substrate interactions and solvent structure alter interfacial solvent polarity from bulk solution limits. Not surprisingly, weakly associating systems consisting of polar substrates and nonpolar solvents are more polar than bulk solution, although there exist subtle, solvent-dependent differences in the strength of interfacial solvent−solute interactions. These differences are attributed to a solvent's ability to pack against a rigid wall. Measurements of solute orientation at weakly associating interfaces supports a model in which the solute experiences multiple interactions with the substrate and adopts an orientation that is deflected significantly from the surface normal. Solvent polarity across strongly associating interfaces depends sensitively on solvent structure. Interfaces formed between hydrophilic silica substrates and *n*-alcohol solvents are significantly less polar than bulk solution, but branched alcohols create regions of enhanced local polarity. These effects are discussed in terms of the substrate's ability to induce long-range structure in the adjacent solvent through hydrogen-bonding interactions. Again, orientation measurements support the interfacial polarity results. In strongly associating systems, interfacial solutes adopt an orientation that is consistent with simulation predictions of alkyl chain tilt angles at extended solid surfaces.

I. Introduction

Chemistry at solid/liquid interfaces forms the cornerstone of innumerable processes ranging from environmental remediation[1,2] to biomineralization[3−5] to bond activation catalysis.[6−9] Numerous experimental and theoretical studies have shown how an imbalance in long-range forces alters interfacial solvent properties from bulk solution limits.[10−16] Considerably less is known about how these changes affect interfacial solvation. Here, solvation refers to the noncovalent interactions experienced between a solute and its surroundings. Surface-mediated solvation will control solute concentration, conformation, and reactivity within the interfacial region. Thus, understanding how interfacial anisotropy affects solvent−solute and solute−surface interactions is essential for formulating quantitative, predictive models of surface chemistry at solid/liquid boundaries. In this work we use second harmonic generation (SHG)[17,18]—a surface specific, nonlinear optical technique that is sensitive to solute electronic structure—to probe solvent polarity at different solid/liquid interfaces. Results show that substrate−solvent interactions strongly influence the local dielectric properties around a solute. However, solvent molecular structure also plays an important role in controlling the interfacial dielectric environment. We attribute these experimental observations to a solid surface's ability to enhance long-range order that extends multiple solvent diameters into solution.[19−22]

Intuitively, one expects solvent polarity at surfaces to differ from bulk solution limits due to interfacial anisotropy. Previous experimental studies of interfacial solvation characterized solvent polarity at interfaces formed between weakly associating, immiscible liquids (e.g., water/cyclohexane).[23,24] The model of interfacial polarity that emerged from second-order nonlinear optical experiments was that of an interface whose dielectric properties reflected simple, averaged contributions from the two adjacent phases.[23,24] While the observed result may seem surprising given the asymmetry inherent to interfacial regions, the result can be understood in terms of a liquid/liquid interface that is both (a) molecularly sharp—properties of one phase converge to those of the other in only a few solvent layers—and (b) microscopically flat—very little thermal roughening on the molecular scale due to capillary wave activity.[25−28] Such a picture is consistent with simulations describing the interfacial properties between an aqueous solvent and a nonpolar, hydrocarbon solvent, although the authors note that calculated effects are very sensitive to interfacial topography *and* the position of the probe relative to the interfacial boundary.[25−28]

Other studies have suggested that the "average-polarity" model breaks down when the adjacent organic solvent is polar (but aprotic).[29,30] Specifically, interfacial polarity inferred from fluorescence measurements at polar organic−aqueous interfaces is considerably less than predicted by the average polarity model. This result could indicate an interface that is either molecularly diffuse or thermally roughened, although simulations predict that a roughened interface should be *more polar* or *not less*

[†] Chemical Physics Program.
[‡] Department of Chemistry and Biochemistry.

10.1021/jp021071i CCC: $25.00
Published on Web 03/18/2003

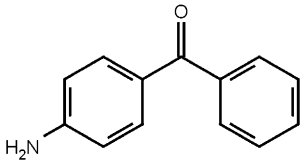

Figure 1. Chemical structure of 4-aminobenzophenone. Ab initio calculations show that in the ground electronic state, the unsubstituted phenyl ring is aligned perpendicular to the amino-substituted ring. The transition moment of the lowest lying $\pi-\pi^*$ (=charge transfer) transition lies along the molecular *a* axis which extends from the nitrogen to the carbonyl bond.

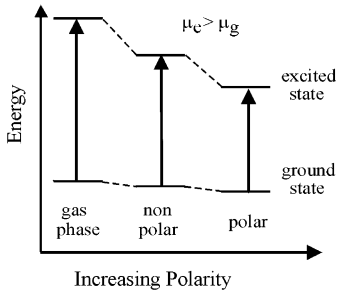

Figure 2. Schematic diagram illustrating the origin of bathochromic solvatochromism. Given a molecular dipole that is larger in the excited electronic state than in the ground state, differential solvation effects will shift the electronic transition energy to longer wavelengths relative to the gas-phase limit. This effect becomes more pronounced as solvent polarity increases.

polar than a molecularly flat boundary.[26,27] Further complicating interpretation of the fluorescence results is the fact that the technique is not surface specific, meaning that even under total internal reflection conditions, experiments still sample up to tens of nanometers into the adjacent, low-index phase. In contrast, second-order nonlinear optical experiments *are* surface specific, with signals originating only within the anisotropic boundary between two isotropic media.

Solid/liquid interfaces promise to differ considerably from their liquid/liquid counterparts. Solid surfaces present rigid boundaries to an adjacent solvent and gradients in chemical potential cannot lead to interphase mixing as can happen in liquid/liquid systems.[29,30] Furthermore, solid surfaces can induce enhanced structure in the adjacent solvent. Depending on the solvent−solvent and solvent−substrate forces, structure in calculated density profiles can extend multiple solvent diameters away from the hard wall.[19−22,31] Such interfacial solvent structure can enhance solvent−solute interactions, thereby increasing the effective solvent polarity experienced by interfacial solute species.[32,33] Evidence of such "solid-like" ordering also can be inferred from time-resolved measurements of solvent relaxation that report substantially slower solvent relaxation times at solid/liquid interfaces relative to bulk solution.[34−36]

The work described below examines how polar, solid surfaces alter the interfacial polarity of adjacent solvents as evidenced by solvatochromic shifts in an adsorbed solute's electronic excitation energy. Experiments use surface-specific, nonlinear optical methods to record effective excitation spectra of 4-aminobenzophenone (4ABP, Figure 1) adsorbed to different solid/liquid interfaces. Comparing the SH excitation maxima of 4ABP adsorbed to solid/liquid interfaces to excitation maxima in corresponding bulk solvents enables us to infer how polar, silica surfaces alter interfacial solvent polarity from isotropic, bulk limits. We find that interfacial solvent polarity depends both on solvent−substrate interactions and solvent molecular structure. We interpret these results based on factors that influence surface-mediated solvent structure: not only can surfaces enhance local solvent density but surfaces can also lead to the formation of anisotropic regions having properties that reflect neither those of the surface nor those of the solvent.

II. Experimental Section

A. General Considerations. - Interfacial Characterization and Solvent Polarity. Solid/liquid interfaces in this work are categorized as either strongly or weakly associating. Strongly associating solid/liquid systems are characterized by strong, hydrogen-bonding interactions between the two phases, while weakly associating systems describe nonpolar solvents adjacent to polar, silica substrates. Previous studies have shown how substrate−solvent interactions significantly impact interfacial solvation.[37,38] Specifically, strongly interacting systems create discrete regions of reduced solvent polarity relative to anticipated contributions from both the substrate and the solvent.[38] Furthermore, the disparity between the solvent−substrate and intrasolvent forces at hydrophobic surfaces leads to regions of significantly reduced solvent polarity, consistent with proposed models of dry-layer formation.[37]

While there exists no rigorous definition of solvent polarity, we choose to describe this property in terms of the averaged, equilibrium electric field experienced by a solute due to polarization of its surrounding solvation shell.[39,40] We employ this Onsager-based description of solvation because of its widespread use in solvation literature and its simple, physically appealing interpretation.[41,42] The field induced within the solute cavity can affect a solute's electronic and nuclear structure. Consequently, solvent-dependent shifts in solute excitation and emission energies can serve as sensitive indicators of local solvent polarity. (Figure 2) When relevant, dipolar interactions between the solvent and solute are thought to be the dominant contribution to a solute's solvatochromic behavior.[43,42] However, a recent, thorough examination of two common empirical solvation scales suggests that dispersion forces may play a more important role in solvation than previously believed.[44]

Measurements of interfacial polarity in this work characterize the local dielectric environment by using the Onsager polarity function, $f(D)$,[39]

$$f(\mathrm{D}) = \frac{2(D-1)}{2D+1} \tag{1}$$

where D is a bulk solvent's static dielectric constant. A solvent's static dielectric constant arises from average local field corrections to the polarization of a solute due to an oscillating external field and can be described in terms of dipolar interactions between the solute and total electric moment of the surrounding medium.[45] The function $f(D)$ has limiting values of ∼0.4 for alkanes and ∼1 for polar liquids such as water (=0.98). In contrast to the numerous empirical scales of solvent polarity (i.e., ET30, π^*),[46−48] $f(D)$ can be related to the nonspecific solvent−solute interactions and can be modified to describe the solvation of solute chromophores having point dipoles.[49,50] We prefer this measure of local polarity over existing empirical solvent polarity scales because it best illustrates the observed nonadditive behavior of local polarity across different solid/liquid boundaries.

Using $f(D)$ as the measure of interfacial solvent polarity also has drawbacks. First, $f(D)$ arises explicitly from a dielectric

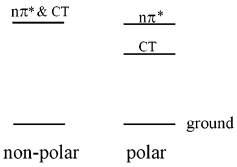

Figure 3. Qualitative representation of the solvent-dependent, electronic state energies of 4ABP in both nonpolar and polar solvents. As discussed in the text, the CT state is primarily responsible for the observed resonance-enhanced signal in the second harmonic spectra.

continuum description of solvent behavior.[42,51] This treatment of solvent−solute interactions assumes that isotropic long-range forces are responsible for local polarity and may not adequately account for surface-induced structural inhomogeneities. Second, $f(D)$ cannot account for static electric fields such as surface potentials that can impact the interfacial dielectric environment sampled by adsorbed solutes.[45] Finally, $f(D)$ is formulated to describe solvation of nonpolarizable spherical solutes having point dipoles. Accounting for polarizable solutes having nonspherical shapes requires geometric corrections and additional adjustable parameters.[49,50] In section IV, we discuss the limitations of using the Onsager reaction field to characterize interfacial solvation and consider possible contributions from surface-mediated, nonadditive dispersion effects.

B. Electronic Structure of 4-Aminobenzophenone (4ABP) and Excited State Solvent Sensitivity. The probe of interfacial solvation used in these studies, 4-aminobenzophenone (4ABP), has two low-lying excited electronic states corresponding to n−π* and π−π* transitions.[49,50] (Figure 3) The n−π* transition transfers ∼0.3 e^- charge from the carbonyl oxygen lone pair to a π* orbital localized across the carbonyl group.[42] Such a small change in electron density leads to a small change in molecular dipole and a small change in molecular hyperpolarizability. The π−π* transition is best represented by a 0.8 e^- charge transfer from the amino-substituted aromatic ring to the carbonyl oxygen.[42,52] Due to the significant change in the electron density, this π−π* transition is commonly referred to the charge-transfer (CT) band.[42,52] The difference in dipole moments between the ground and CT state is ∼7.9 D, clearly reflecting the transition's CT character.[42] 4ABP was chosen as a probe of interfacial solvation due to the sensitivity of the CT excitation energy to solvent polarity. (Figure 3).

Although 4ABP rapidly undergoes internal conversion to a triplet state upon photoexcitation, solute photoreactivity is not of concern for two reasons. First, unlike hydroxy substituted benzophenones that extract hydrogen atoms from surrounding solvent species with near unit efficiency, amino-substituted benzophenones are remarkably unreactive in their excited states.[52] This photochemical stability of the T_1 state has been attributed to resonance stabilization arising from multiple electronic configurations that place a formal negative charge (rather than a single electron radical) on the ketone functional group.[52] The second reason that 4ABP photoreactivity need not be considered in the experiments examining interfacial polarity is that the nonlinear optical methods employed do not actually lead to photoexcitation of the interfacial chromophores.[53,54] Rather, experiments exploit the resonance enhancement in 4ABP's hyperpolarizability to generate the observed second harmonic signal in a coherent scattering process. The solute never spends any time on the excited-state surface.

C. Measures of Solvent Polarity. With such a large change in permanent dipole, the $\pi\angle\pi$* transition of 4ABP is particularly sensitive to the local solvent polarity. The large increase in permanent dipole leads to preferential solvation of the excited-state potential energy surface relative to the ground-state surface[42] (Figure 2). In bulk solution, the CT excitation wavelength (λ_{max}) shifts ∼35 nm as solvent polarity increases from that of alkanes (λ_{max} ∼ 300 nm) to that of short-chain alcohols and water (λ_{max} ∼ 336 nm) (Figure 4). This behavior is known as bathochromic solvatochromism.[55] The data shown in Figure 4 could be represented in a number of ways. Plotting 4ABP excitation maxima versus an empirical polarity scale (such as π* or ET(30)) would result in a more linear fit but would not shed any additional insight into 4ABP's behavior in bulk solution. Furthemore, the ET(30) scale is ill equipped to accommodate solvent−solute interactions such as hydrogen bonding, and the alcohol solvents all have almost equivalent π* values by virtue of 4ABP having similar excitation maxima in polar, protic solvents (Table 1). Thus, to distinguish between different linear and branched alcohols, we choose to plot the 4ABP excitation maxima in various solvents vs the Onsager function, f(D). The quality of the linear fit in Figure 4 is not of concern as this work focuses on shifts in the SH excitation maxima of 4ABP solutes adsorbed to different solid/ liquid interfaces *relative to excitation maxima in bulk solutions*. Based on whether a specific solid/liquid combination shifts the 4ABP spectrum to shorter or longer wavelengths, we can infer how

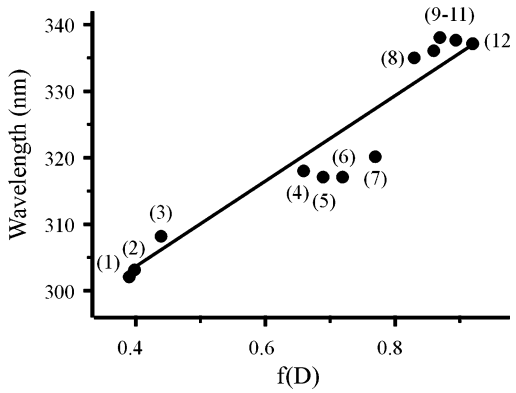

Figure 4. Solvatochromic behavior of 4ABP in a variety of solvents. Data correspond to bulk solution excitation maxima of 4ABP plotted vs the Onsager polarity function, $f(D)$. See text for details. Solvents: (1) isooctane; (2) cyclohexane; (3) carbon tetrachloride (CCl_4); (4) diisopropyl ether; (5) diethyl ether; (6) chloroform; (7) ethyl acetate; (8) 1-decanol; (9) 1-octanol; (10) isobutanol; (11) 1-hexanol and 1-pentanol; (12) 1-butanol, 1-propanol, and 2-propanol.

TABLE 1: Excitation Maxima Of 4ABP Dissolved In Various Solvents And SHG Maxima of 4ABP Adsorbed to Different Hydrophilic Silica/Solvent Interfaces[a]

solvent	ϵ[b]	$f(D)$	λ_{max}(UV), nm	λ_{max}(SHG), nm	$\Delta\lambda$, nm
1-propanol	20.1	0.93	337	332 ± 1	−5
1-butanol	17.5	0.92	337	330 ± 1	−7
1-pentanol	13.9	0.9	337	331 ± 2	−6
1-hexanol	13.3	0.89	338	331 ± 1	−7
1-octanol	10.3	0.86	336	326 ± 1	−10
1-decanol	8.1	0.83	335	324 ± 2	−11
2-propanol	18.3	0.92	336	339 ± 2	+3
isobutyl alcohol	10.9	0.87	338	339 ± 1	+1
diisopropyl ether	3.88	0.66	318	326 ± 2	+8
carbon tetrachloride	2.2	0.44	308	329 ± 1	+21
cyclohexane	2.02	0.40	303	318 ± 1	+15

[a] Data were determined according to procedures described in text. Also listed are static dielectric constants and associated Onsager polarity values for the various solvents. [b]Data from ref 74 (at 20 °C).

the surface has either inhibited or promoted solute−solvent and solute-substrate interactions.

D. Surface Specific Spectroscopy. Second Harmonic Generation (SHG). Given experimental requirements of molecular sensitivity and surface specificity, second harmonic generation (SHG) spectroscopy stands out as an ideal technique for examining interfacial solvation.[17,18,56,57] SHG spectroscopy can detect the resonance response of adsorbed chromophores with less than 10% of full monolayer coverage, and the origin of the second harmonic response makes the technique inherently surface sensitive within the electric dipole approximation.[58,59]

SHG originates from the second-order polarization induced by strong oscillating electric fields. The induced second-order polarizability is proportional to the square of the amplitude of the impinging field:

$$P^{(2)} = \chi^{(2)}E^2(\omega) \tag{2}$$

where $\chi^{(2)}$ is the second-order susceptibility, a third rank tensor. The $\chi^{(2)}$ tensor contains 27 elements, and symmetry considerations require that each element changes sign under inversion:

$$\chi^{(2)}(x,y,z) = -\chi^{(2)}(-x,-y,-z) \tag{3}$$

Within the electric dipole approximation, this condition forces $\chi^{(2)}$ to be zero in isotropic media. At interfaces, however, inversion symmetry is broken and a second-order response is allowed. The second harmonic intensity $I(2\omega)$ is equal to the square of the SHG signal field,

$$I(2\omega) = E^2(2\omega) \tag{4}$$

and the SHG signal field is proportional to the second-order polarizability, $P^{(2)}$:

$$I(2\omega) = E^2(2\omega) \propto |P^{(2)}|^2 = |\chi^{(2)}|^2 E^4(\omega) = |\chi^{(2)}|^2 I^2(\omega) \tag{5}$$

where $I(\omega)$ is the intensity of the incident field. If the SHG signal comes from an interface that is rotationally invariant around the surface normal (i.e., isotropic in plane distribution), $\chi^{(2)}$ has only three unique, nonzero elements: χ_{zzz}, χ_{xxz} ($=\chi_{xzx}$), and χ_{zxx}.[18,23,60,61] Each $\chi^{(2)}$ element contains contributions from both nonresonant and resonant terms:

$$\chi^{(2)} = \chi_{\mathrm{nr}}^{(2)} + \chi_{\mathrm{r}}^{(2)} \tag{6}$$

In principle, resonant and nonresonant terms can add constructively or destructively leading to asymmetric band shapes. However, for dielectric systems such as those discussed below, the resonant term is several orders of magnitude larger than the nonresonant contribution, meaning that $\chi^{(2)}{}_{\mathrm{nr}}$ can be treated as a small perturbation to the observed response. The resonant terms $\chi^{(2)}{}_{\mathrm{r}}$, can be related to the corresponding microscopic hyperpolarizabilities, β_{ijk}:[56,18]

$$\chi_{xyz}^{(2)} = N_{\mathrm{s}}\sum_{ijk}\langle(\hat{\mathrm{x}}\cdot\hat{\mathrm{i}})(\hat{\mathrm{y}}\cdot\hat{\mathrm{j}})(\hat{\mathrm{z}}\cdot\hat{\mathrm{k}})\rangle\beta_{\mathrm{ijk}}^{(2)} \tag{7}$$

where N_{s} is the density of the molecules adsorbed to the surface, (X,Y,Z) and (i,j,k) are unit vectors along the lab and the molecular coordinate, respectively. The elements of β are given by[56,18]

$$\begin{aligned}\beta_{ijk} + \beta_{ikj} = \frac{-e^3}{4\hbar^2}\sum_{n,n'=g}^{N} &(r_{gn'}{}^{j} r_{n'n}{}^{i} r_{ng}{}^{k} + r_{gn'}{}^{k} r_{n'n}{}^{i} r_{ng}{}^{j})\left(\frac{1}{(\omega_{n'g} - \omega + i\Gamma_{n'g})}\frac{1}{(\omega_{ng} + \omega - i\Gamma_{ng})} + \frac{1}{(\omega_{n'g} + \omega + i\Gamma_{n'g})}\frac{1}{(\omega_{ng} - \omega - i\Gamma_{ng})}\right) + (r_{gn'}{}^{j} r_{n'n}{}^{i} r_{ng}{}^{k} + \\ &r_{gn'}{}^{k} r_{n'n}{}^{k} r_{ng}{}^{j})\left(\frac{1}{(\omega_{n'g} + 2\omega - i\Gamma_{n'g})}\frac{1}{(\omega_{ng} + \omega - i\Gamma_{ng})} + \frac{1}{(\omega_{n'g} - 2\omega - i\Gamma_{n'g})}\frac{1}{(\omega_{ng} - \omega - i\Gamma_{ng})}\right) + (r_{gn'}{}^{j} r_{n'n}{}^{k} r_{ng}{}^{i} + \\ &r_{gn'}{}^{k} r_{n'n}{}^{k} r_{ng}{}^{i})\left(\frac{1}{(\omega_{n'g} - \omega - i\Gamma_{n'g})}\frac{1}{(\omega_{ng} - 2\omega + i\Gamma_{ng})} + \frac{1}{(\omega_{n'g} + 2\omega + i\Gamma_{n'g})}\frac{1}{(\omega_{\mathrm{ng}} + 2\omega + i\Gamma_{ng})}\right)\end{aligned} \tag{8}$$

where ω is the incident laser frequency; $r_{nn'}{}^{i}$ is the transition dipole matrix between state n and state n' and $r_{nn'}{}^{i} = \langle Y_n|r^i|\Psi_{n'}\rangle$; hw is the energy difference between the state n and state n'; Γ_{ng} is the lifetime of excited-state n. In a later section, the relevant β_{ijk} terms of 4ABP are calculated using semiempirical methods.[62−66] The results are then used to evaluate the magnitude of different $\chi^{(2)}$ elements and, subsequently, solute orientation at weakly and strongly associating solid/liquid interfaces.[17,18,60]

An important aspect of eq 8 is that when 2ω is resonant with ω_{ng}, β (and hence $\chi^{(2)}$) becomes large, leading to a strong resonance enhancement in the observed intensity at 2ω. Thus, measuring the scaled intensity $[I(2\omega)/I^2(\omega)]$ as a function of 2ω records an effective excitation spectrum of solutes adsorbed to the solid/liquid interface. Reported SHG spectra are resonantly enhanced when 2ω matches the energetic separation between the ground and excited state. The observed SHG response arises from a coherent scattering event that becomes more efficient when $2\omega = \omega_{\mathrm{ng}}$, not from an actual optical transition that leaves 4ABP in an excited electronic state.

E. Experimental Details. Excitation spectra of 4ABP in various bulk solvents were recorded with a Hewlett-Packard 8452A diode array spectrophotometer with 1-nm resolution. Bulk concentrations were adjusted so that absorbance levels never exceeded 0.9, thus ensuring that saturation effects did not perturb band profiles and positions. In addition, the observed insensitivity of band position and band profile to solute concentration indicates that solute dimerization/aggregation did not play a role in solution. The excitation maxima of 4ABP in bulk solvents were obtained from fits of the UV−vis spectra to two Gaussian features corresponding to the n−π* and $\pi-\pi$* transitions.[42,52] Results show that one feature remains centered at ∼288 nm, while the other transition red shifts by ∼35 nm as solvent polarity increases. These observations are consistent with the electronic structure of 4ABP (Figure 3). All solvents (typically HPLC grade) and 4ABP were purchased from Aldrich and used without further purification.

All reported SHG spectra resulted from solutions that were saturated or almost saturated in 4ABP. However, for each specific solvent−substrate system, experiments were carried out over a range of solute concentrations, and resulting SHG spectra

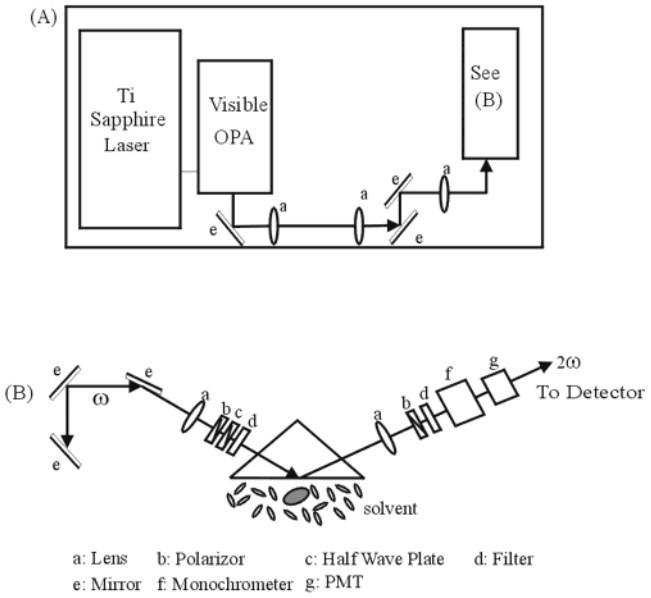

Figure 5. Experimental setup for second harmonic generation experiment.

showed no detectable variation in band position or band profile, indicating that interfacial solute−solute interactions did not play a significant role in perturbing interfacial dielectric properties. For strongly associating systems, simple stoichiometric considerations predict solute concentrations of less than 10% of a close-packed monolayer. Solute surface concentrations at weakly associating interfaces will be higher, but spectra still show no evidence of solute−solute interactions. Solid/liquid interfaces were created by placing a fused silica prism (Edmund Industrial Optics) hypotenuse side down onto a Teflon cell containing a reservoir of solution. Prior to use, prisms were cleaned in a 50:50 mixture (by volume) of concentrated sulfuric and fuming nitric acid at elevated temperature (∼60−75 °C). Prisms cleaned in this manner always exhibited complete wetting (e.g., zero degree contact angle) by an aqueous solvent.

The SHG apparatus used is shown in Figure 5. A Ti:sapphire regeneratively amplified, femtosecond laser (Clark-MXR CPA2001) produced 130-fs pulses with energies of ∼700 μJ at a wavelength of 775 nm with a repetition rate of 1 kHz. The output of the Ti:sapphire laser pumped a commercial optical parametric amplifier (OPA, Clark-MXR). The visible output of the OPA was tunable from 560 to 700 nm, with a bandwidth of 2.5 ± 0.5 nm. Incident energies ranged from 0.1 to 0.8 μJ/pulse. The polarization of the incident beam is controlled with a Glan-Taylor polarizer and a half-wave plate. A series of filters blocked the fundamental at 775 nm and any second harmonic light generated from the preceding optical components. Second-harmonic photons were detected in the reflected direction by using photon-counting electronics. Typical signal levels averaged 0.01−0.1 photons per shot. The second polarizer selects the polarization of the SHG signal. A short pass filter and monochromator served to separate the second-harmonic signal from background radiation.

Because the visible OPA cannot be synchronously tuned, acquisition of a complete SHG spectrum typically required several hours. Standard procedure entailed letting the solid/liquid system equilibrate (as evidenced by an unchanging SHG intensity), followed by manually tuning ω_{vis} to each desired wavelength. System alignment was reoptimized at every wavelength to account for the wavelength-dependent refractive indices of the prism and collection optics. At each wavelength, SHG data were collected for three 10-s intervals and normalized

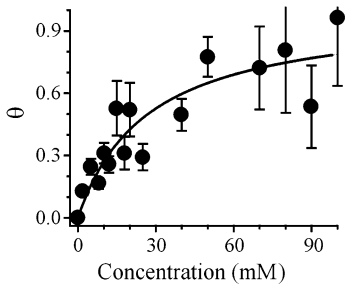

Figure 6. Relative coverage (θ) of 4ABP on hydrophilic silica slide plotted vs 4ABP concentration in bulk methanol. See text for details of sample preparation and data acquisition. Solid line corresponds to fitting the data to a Langmuir isotherm. Low concentration data can be used to calculate ΔG_{ads}.

for incident power. Although tedious, this procedure ensured that spectra were reproducible. A single wavelength might be sampled three separate times, several hours apart (beginning, middle, and end of acquisition sequence). If the normalized SHG signal from each of these three samples did not fall within the limits of experimental uncertainty (typically <15%), data acquisition was halted and the spectrum discarded. Furthermore, data at the same wavelength were often acquired at several different incident powers and then normalized to confirm the quadratic dependence of SH signal intensity on the incident field intensity predicted by eq 5. Predicted quadratic behavior was always observed.

Acid−base reactivity between the surface silanol groups and the primary amine of 4ABP represented a potential source of reactive instability. Full silanol coverage of a polycrystalline silica surface leads to surface coverages of 5.0 OH groups per nm^2.[67] Approximately 20% of these silanol groups have a pK_a of 4.5, while the remaining 80% exhibit a pK_a of 8.5.[68,69] In principle, the acidic SiOH group can donate a proton to adsorbed 4ABP solutes.

$$RNH_2 + -SiOH \rightarrow RNH_3^+ + -SiO^- \qquad (9)$$

Deprotonation of the surface silanol groups can generate a large surface potential leading to tremendous enhancements of the interfacial nonlinear polarizability.[68] Furthermore, protonation of the interfacial 4ABP species alters the solute's electronic structure, rendering the $\pi-\pi^*$ charge-transfer state inaccessible. Bulk studies of 4ABP in acidic solutions show a single, weak excitation at ∼385 nm. Assuming a representative pK_b of ∼9 for the $-NH_2$ group of 4ABP, simple equilibrium considerations predict the concentration of charged species to be approximately equal to that of the neutral, adsorbed 4ABP. However, SHG experiments show no evidence of either a charged interface or a protonated solute species. We attribute this disparity between predicted acid−base equilibrium and experimental observations to our use of nonaqueous solvents. While the systems studied undoubtedly have trace amounts of water present, surface silanol and solute acid dissociation constants do not accurately describe observed interfacial behavior.

III. Results

A. Surface Activity for Polar Protic and Aprotic Liquid/Solid Systems. Strong hydrogen bonding interactions between surface silanol groups and the primary amine of 4ABP are responsible for solute surface activity. Figure 6 shows the adsorption isotherm for 4ABP to a hydrophilic silica surface from methanol solutions. Data represent UV absorbance measurements acquired from silica slides that had been submerged

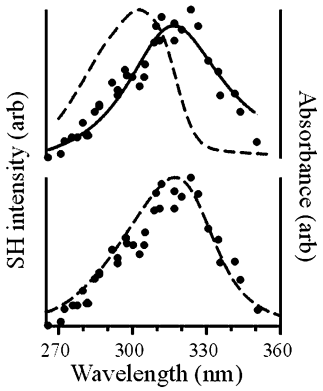

Figure 7. Top panel: Excitation spectra of 4ABP in bulk cyclohexane (dashed line) and SHG spectra of 4ABP adsorbed to the hydrophilic solid/cyclohexane interface. The solid line through the second harmonic spectrum represents the best fit to the data according to eqs 6−8. Bottom panel: Spectrum of 4ABP in bulk ethyl ether (dashed line) overlaid with the surface spectrum of 4ABP adsorbed to the hydrophilic solid/cyclohexane interface. The SHG spectra in the upper and lower panels are identical. SHG spectra were recorded under $P_{in}P_{out}$ conditions.

in 4ABP/methanol solutions of varying concentrations. After allowing sufficient time for equilibration, slides were slowly removed from solution, and the excess solution was allowed to run to the bottom of the slide. UV absorbance spectra were acquired in a transmission geometry at normal incidence. Multiple spectra were acquired from several positions toward the top of the slide where multilayer formation would be minimized.[18,70−72] Error bars provide a measure of reproducibility in surface coverage. A quantitatively similar isotherm resulted from solutions of 4ABP in acetonitrile. Isotherms from less volatile solvents were difficult to acquire due to multilayer buildup and inhomogeneous film formation.

This method of measurement assumes that adsorbed solutes have some component of their transition moment oriented parallel to the surface and that the adsorbed solutes do not undergo a surface concentration dependent change in their average orientation or electronic structure.[73] Measurements of solute orientation at these hydrophilic surfaces confirm that the solutes do, in fact, have a significant component of their transition moment aligned parallel to the surface (vide infra), and solvatochromic SH experiments do not show any evidence of interfacial solute aggregation. Although noisy, the UV absorbance data fit reasonably well to a Langmuir isotherm.[74] The slope of the isotherm at low 4ABP concentrations leads to a calculated adsorption free energy $\Delta G_{ads} = -16 \pm 1$ kJ/mol. This value compares favorably with one hydrogen bond being formed per monomer adsorption.[75] Adsorption energies of alcohols to silica surfaces are ~ -17 to -20 kJ/mol, again implying that hydrogen bonding is the primary driving force of 4ABP adsorption. In principle, the primary amino group in 4ABP can form two or three hydrogen bonds with surface silanol groups (two as a hydrogen bond donor, one as a hydrogen bond acceptor). The fact that adsorption data are consistent with only one H-bond being formed between the solute and surface suggests that the additional solute hydrogen bonding sites go unutilized probably due to the steric limitations between the substrate and the solute. The surface itself presents a nucleophilic environment due to the oxygen electron lone pairs,[75] so the solute−substrate hydrogen bonding probably occurs through the amino N−H bond.

B. Solvent Polarity at Weakly Associating Hydrophilic Solid/Nonpolar Liquid Interfaces. Figure 7 shows the $P_{in}P_{out}$ SHG spectrum of 4ABP adsorbed to a hydrophilic silica surface

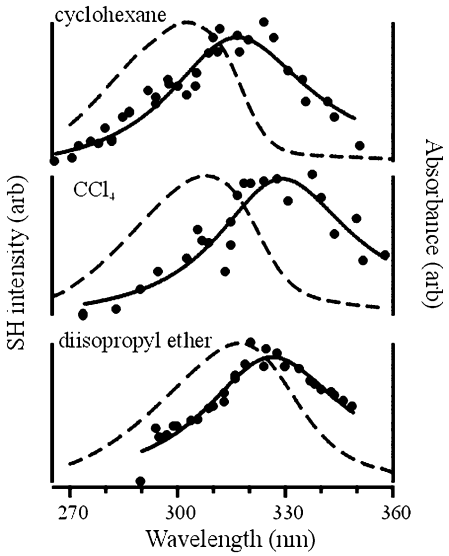

Figure 8. Spectra of 4ABP in different bulk solutions (dashed lines) and adsorbed to different solid/liquid interfaces (points) and fits to the different sets of SHG data (solid lines). Data are shown for the hydrophilic solid/cyclohexane interface (top panel); the hydrophilic solid/carbon tetrachloride interface (middle panel); and the hydrophilic solid/diisopropyl ether interface (bottom panel). Fits were generated according to eqs 6−8. Spectra were recorded under $P_{in}P_{out}$ conditions for the visible and second harmonic fields, respectively.

from a solution of 4ABP in cyclohexane. The SHG data were fit to single electronic resonance according to eqs 6−8. Contributions from the n−π* resonance were neglected due to the transition's very small contributions to the solute's hyperpolarizability. Superimposed are UV−vis spectra (dashed line) of 4ABP in bulk cyclohexane (upper panel) and bulk diethyl ether (bottom panel). Compared to its excitation spectrum in bulk cyclohexane, the spectrum of 4ABP adsorbed to a cyclohexane/hydrophilic interface shifts to longer wavelengths by 15 nm. Together with 4ABP's solvatochromic behavior shown in Figure 4, the data imply a more polar interfacial environment relative to bulk cyclohexane. This observation affirms intuition: the interfacial boundary between a polar substrate and a nonpolar solvent *should* be more polar than bulk solution. Empirically, the data show that the local polarity sampled by 4ABP at the silica/cyclohexane interface is very similar to that of bulk diethyl ether ($\epsilon = 7.69$, $f(D) = 0.69$) (Figure 7, lower panel).

Data from additional weakly associating solid/liquid systems confirm that surface dipoles render the interfacial environment more polar than bulk solution. The top panel of Figure 8 shows the same bulk and surface spectra of 4ABP in cyclohexane that appear in Figure 7. The bottom panel of Figure 8 shows the spectra of 4ABP in bulk diisopropyl ether and adsorbed to the ether/silica interface. The spectrum of 4ABP adsorbed to the ether/hydrophilic interface red shifts relative to bulk solution, but the shift in this system is only 8 nm—half that of the cyclohexane/hydrophilic system. Diisopropyl ether can serve as hydrogen bond acceptor for surface silanol groups, but such interactions are weak given the in-plane orientation of the OH bond and the high electronic density at the silica surface.[75]

Curiously, the SHG spectrum of 4ABP adsorbed to the hydrophilic solid/CCl_4 interface shifts 21 nm to a longer wavelengths relative to bulk CCl_4 solution. (Figure 8, middle panel). Cyclohexane and CCl_4 have almost identical dielectric constants and polarizabilities ($\epsilon_{chex} = 2.02$, $\epsilon_{CCl_4} = 2.23$, $\alpha_{chex} = 11.0 \cdot 10^{-24}$ cm^{-3}, $\alpha_{CCl_4} = 11.2 \times 10^{-24}$ cm^{-3}).[76] Excitation maxima of 4ABP in these two solvents differ by 5 nm. This

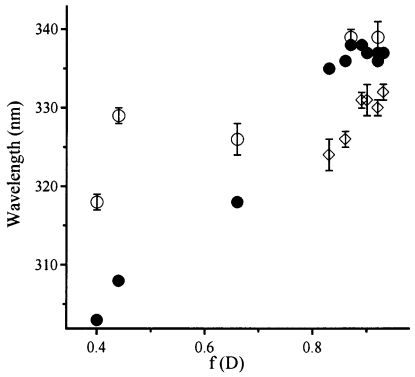

Figure 9. Composite showing bulk solution excitation maxima (dots) and SH excitation maxima of 4ABP adsorbed to different hydrophilic solid/solvent interfaces (diamonds) plotted vs solvent polarity. Open diamonds depict SH excitation maxima for *n*-alcohol solvents. All other SH excitation maxima are represented with open circles. Error bars correspond uncertainties in fitting the SHG data according to eqs 6−8. All spectra were recorded under $P_{in}P_{out}$ conditions. From left to right, solvents correspond to (1) cyclohexane, (2) CCl_4, (3) diisopropyl ether, (4) 1-decanol, (5) 1-octanol, (6) isobutanol, (7) 1-hexanol, (8) 1-pentanol, (9, 10) 1-butanol and 1-propanol, and (11) 2-propanol.

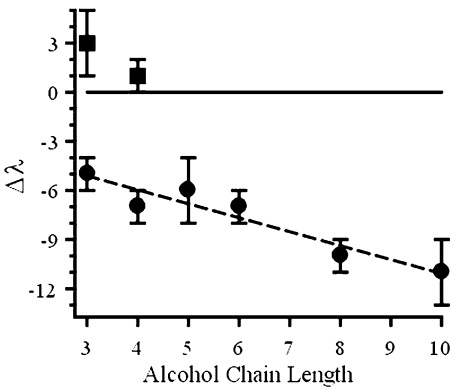

Figure 10. Differences in 4ABP absorption maxima between bulk solution and solid/liquid interface for various alcohol solvents plotted vs number of carbon atoms in solvent structure. Circles correspond to *n*-alcohols (1-propanol up to 1-decanol), while squares correspond to branched alcohols. Negative differences ($\Delta\lambda < 0$) indicate an interfacial environment that is less polar than the bulk solution, while positive differences denote an interface that is more polar than the bulk solution. Note that plotted this way, variations in different solvent dielectric properties do not influence the data because each point is referenced to the behavior of 4ABP in each individual solvent.

difference arises from the more efficient packing of the smaller spherical CCl_4 solvent molecules around the solute. Simple molecular volume considerations show that 4ABP is surrounded by 10−15% more partners when solvated in CCl_4 compared to cyclohexane. The hydrophilic surface appears to further enhance interfacial CCl_4 polarity relative to the equivalent hydrophilic solid/cyclohexane boundary, as evidenced by the more pronounced red shift of the interfacial spectrum of 4ABP dissolved in CCl_4 compared to cyclohexane solution. We address this issue in the section IV and attribute the disparity to differences in solvent shape and surface-induced gradients in solvent density against a rigid wall.

C. Solvent Polarity at Strongly Associating Hydrophilic Solid/*n*-Alcohol Liquid Interfaces. Spectra from the solid/cyclohexane and solid/CCl_4 systems already suggest that solvent polarity across solid/liquid interfaces does not represent averaged contributions from the bulk solvent and the hydrophilic surface. An examination of *strongly* associating solid/liquid interfaces reinforces this view. Figure 9 presents excitation data from bulk solution and interfaces from 11 different hydrophilic solid/liquid systems. As discussed above, a cursory inspection shows that SHG spectra of 4ABP adsorbed to weakly associating solid/liquid interfaces always show a red shift relative to bulk solutions, but the magnitude of the shift varies. Qualitatively, the observed behavior supports the idea that interfacial solvent polarity represents some sort of weighted average from the two adjacent phases, although how to scale surface and solvent contributions is unclear. For most polar solvents ($f(D) > 0.8$), however, 4ABP SH spectra shift to shorter wavelengths, implying that interfacial solvent polarity is less than in bulk solution. This trend is not universal, though, as some polar solvents having equivalent bulk dielectric properties create more polar environments adjacent to a polar, hydrophilic solid substrate. Data are summarized in Table 1 along with relevant dielectric information for each solvent.

Closer inspection of Figure 9 shows that those solvents responsible for less polar interfacial regions are all *n*-alcohols. Figure 10 depicts the difference in excitation maxima between the bulk solution spectra and interface spectra for linear and branched alcohols. The *n*-alcohol data reveal a consistent trend: the transition energy of 4ABP shifts to shorter wavelengths relative to each solvent's bulk solution limit, meaning that the *n*-alcohol solvents, regardless of the chain length, create an interfacial region that is less polar than bulk solution. The nonpolar environment becomes more pronounced as chain length increases. This observation that a hydrophilic substrate and polar solvent can create *a less polar* interfacial environment may seem surprising given the high density of surface dipoles and the moderate to high dielectric constants of the adjacent solvents.

Earlier studies attributed reduced polarity to the formation of a bilayerlike structure of solvents at the interfaces.[38] The reported surface concentration of silanol groups at a fully hydroxylated surface ($4.8/nm^2$)[67] matches almost exactly the molecular density of long chain alcohols in the tightly packed limits.[77] We believe that substrate-induced polar ordering of the solvent partitions the interface into regions having discrete dielectric properties that vary on molecular length scales. Analogous structures within *n*-alcohol solvents have been observed by X-ray scattering at air/liquid boundaries.[78] Nonlinear optical vibrational studies of *n*-alcohols also suggest that interfacial solvent species pack together in anisotropic monolayerlike structures at air/liquid interfaces.[77]

If solvent−substrate hydrogen bonding is strong enough to inhibit dipolar solvent−solute (and substrate−solute) interactions, the interfacial environment will exhibit decidedly reduced local polarity relative to bulk solution, where solvent molecules can reorient freely around the solute. Given its size, 4ABP can actually span a 1-propanol bilayer, meaning that the effects of bilayer formation on local dielectric properties should be smaller for short-chain alcohols, consistent with the observed data (Figure 9). In contrast, a bilayer consisting of 1-decanol can span ∼3 nm, meaning that 4ABP in the interfacial region can be completely surrounded by alkyl chains. We also note that signal levels in the solvatochromic SH spectra also tended to diminish as alcohol chain length increased. For example, signal levels in 1-butanol systems were 4 times as great as in 1-octanol systems. Given that the substrate in all cases was the same and that the 4ABP bulk concentrations were approximately the same in the *n*-alcohol solvents, differences in observed signal intensity could result either from differences in solute orientation *or* from reduced surface concentrations. In a subsequent section, we report that solute orientation remains unchanged in different strongly associating solid/liquid systems. Thus, we attribute reduced intensity in the SH spectra to lower concentrations of

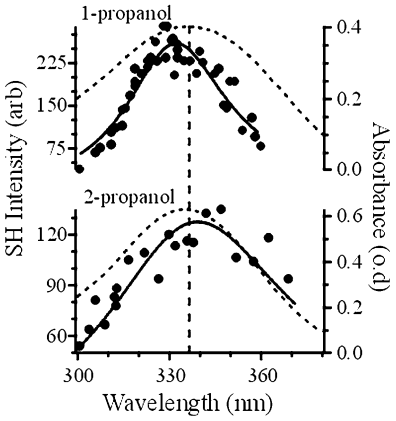

Figure 11. Bulk solution excitation spectra (dashed lines) and SHG surface spectra (points) of 4ABP adsorbed to the silica/1-propanol and silica/2-propanol interfaces. Solid lines correspond to fitting the SHG data according to eqs 6−8. The vertical dashed line denotes the excitation wavelength of 4ABP in both bulk 1-propanol and bulk 2-propanol and is shown to emphasize the qualitative difference in interfacial polarity arising from these two solvents having very similar solution-phase dielectric properties. Spectra were recorded under $P_{in}P_{out}$ conditions.

solute at the interface. This reasoning is also consistent with inhibited substrate/solute interactions arising from surface-induced ordering in the interfacial solvent layer.

D. Solvent Polarity at a Strongly Associating Hydrophilic Solid/Branched Alcohol Interface. Data from Figure 9 show that two solvents having equivalent bulk solution polarity (equivalent $f(D)$) can create decidedly different environments next to hydrophilic solid surfaces. For systems studied thus far, theses differences are most pronounced for linear vs branched protic isomers. Figure 11 shows 4ABP adsorbed to 1-propanol/silica and 2-propanol/silica interfaces. The data clearly show that the interfacial dielectric environment depends on solvent structure. The isomers 1-propanol and 2-propanol have similar dielectric constants at 25 °C (20.1 and 18.3, respectively), similar $f(D)$ values (0.93 and 0.92 respectively), and UV absorption maxima that differ by ≤1 nm. However, the interfacial dielectric environments for the two systems are very different. The SHG spectrum for 4ABP adsorbed to the 2-propanol/hydrophilic interface shows a 3-nm *red* shift, while 4ABP in the 1-propanol/hydrophilic interface shows a 5-nm *blue* shift (Table 1).

Based on bulk dielectric considerations, these results are counterintuitive. The linear 1-propanol is more polar ($\epsilon = 20.1$) than 2-propanol ($\epsilon = 18.3$), yet 1-propanol forms a less polar environment at the hydrophilic surface, while the 2-propanol interfacial region is more polar than bulk solution. Again, we can understand these results based on the extended interfacial solvent structure formed by linear alcohol solvents. 1-Propanol can form a well-ordered tightly packed monolayer with a monomer's cross-sectional area of 21 Å^2/molecule.[74] Branched alcohols cannot pack as efficiently due to steric hindrance. Assuming that 2-propanol hydrogen bonds to the hydrophilic substrate, each 2-propanol monomer occupies ∼60 Å^2/molecule, leaving ∼2/3 of all surface dipoles unscreened and able to interact with adsorbed solutes. These data emphasize the importance of molecular structure and interface interactions in controlling the interfacial solvation properties. Furthermore, these findings also highlight the limitations of using structureless dielectric continuum models to describe interfacial solvation.

E. Polarization Dependence of the SHG Response and Average Molecular Orientation. Resonance-enhanced SHG can be used to probe solute orientation as well as interfacial

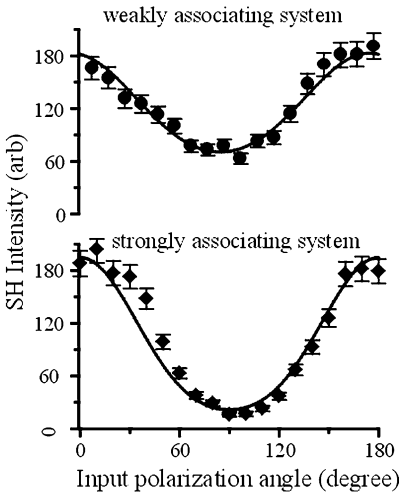

Figure 12. Dependence of the resonant SHG signal from 4ABP on incident angle of ω_{vis} (γ in eqs 10a,b) for a weakly associating system (silica/cyclohexane, top panel) and a strongly associating system (silica/1-butanol, bottom panel). Data for other weakly and strongly associating systems were quantitatively similar. The outgoing SHG field was p-polarized. Solid lines correspond to fitting the data with eq 10b. Data were acquired at wavelengths of 320m for both the weakly associating systems and the strongly associating systems.

TABLE 2: Nonzero $\chi^{(2)}$ Elements (χ_{zzz}, χ_{xzx} (=χ_{xxz}), and χ_{zxx}) and Tilt Angles θ of 4ABP Adsorbed to Four Hydrophilic Silica/Liquid Systems

solvent	χ_{zzz}	$\chi_{zxx}(1)$	$\chi_{xzx}(1)$	$\theta(1)$	$\chi_{zxx}(2)$	$\chi_{xzx}(2)$	$\theta(2)$
cyclohexane	1.0	0.551	0.442	46°	0.665	−0.532	49°
n-hexanedecane	1.0	0.700	0.406	50°	0.836	−0.485	52
1-butanol	1.0	0.297	0.310	38°	0.331	−0.345	39
1-octanol	1.0	0.297	0.585	38°	0.385	−0.758	41

dielectric properties. For SHG signal fields polarized perpendicular to the plane of incidence (S) and parallel to the plane of incidence (P), the SHG signal ($I_s(2\omega)$ and $I_p(2\omega)$, respectively) can be expressed as follows:

$$I_s(2\omega) \propto |a \sin^2(2\gamma)|^2 I^2(\omega) \quad (10a)$$

$$I_p(2\omega) \propto |b \cos^2\gamma + c \sin^2\gamma|^2 I^2(\omega) \quad (10b)$$

where γ is the polarization angle of the incident field relative to the plane defined by the surface normal and the field propagation direction and

$$a = g_1\chi_{xxz} \quad (11a)$$

$$b = g_2\chi_{xxz} + g_3\chi_{zxx} + g_4\chi_{zzz} \quad (11b)$$

$$c = g_5\chi_{zxx} \quad (11c)$$

Here the g_i terms are constants for a fixed angle of incidence. They can be readily evaluated given experimental parameters.[18] The coefficient a can be determined unambiguously by measuring the S-polarized SHG intensity with $\gamma = 45°$ and $b$and c can be deduced by fitting P-polarized SHG intensity versus the polarization of the incident light. Figure 12 shows the P-polarized SHG signal of 4ABP adsorbed to hydrophilic substrate from solutions of cyclohexane and 1-butanol as a function of γ. Given a magnitude of χ_{xxz} from the $M_{in}S_{out}$ (M refers to $\gamma = 45°$) measurement, fitting the data in Figure 12 to eq 10 results in two different sets of nonzero $\chi^{(2)}$ elements (Table 2). The two sets differ in the sign of χ_{xxz} relative to the sign of the major χ_{zzz} element. Confirming the absolute signs of all three elements

requires measuring the phase of the SHG responses relative to the incident field ($E(\omega)$). Analogous measurements have been carried out for air/liquid and air/solid interfaces. Phase-dependent experiments become considerably more difficult when the fields ($E(\omega)$, $E(2\omega)$) pass though a dispersive medium such as a silica prism. Efforts are under way to surmount this experimental challenge. Even without absolute phase data, however, the two sets of $\chi^{(2)}$ elements lead to calculated orientations of 4ABP that are equivalent within experimental uncertainty for each of the systems examined.

Studies of the interfacial solute orientation require that the nonzero elements of the $\chi^{(2)}$ tensor, χ_{zzz}, χ_{xxz} ($=\chi_{xzx}$), and χ_{zxx}, be related to the molecular hyperpolarizability, β. To assess which β_{ijk} elements make significant contributions to the molecular hyperpolarizability, we evaluated the ground and first excited state π-electron wave functions for 4ABP by using the semiempirical Pople−Pariser−Parr (PPP) method.[62−66] In molecules where the low-lying electronic structure is controlled by delocalized π electrons, PPP calculations have produced reasonably accurate results for a wide variety of molecular symmetries.[66,65] Ab initio calculations of excited-state electron density indicated that the second phenyl ring does not participate in the lowest $\pi-\pi^*$ transition, and this group was replaced with a hydrogen atom in the PPP ground and excited-state calculations. The lack of symmetry in 4ABP (and in the 4-aminoacetophenone model used in the PPP calculations) leads to numerous nonzero β_{ijk} elements. However, the two major elements, β_{zzz} and β_{xzz}, account for more than 80% of the total tensor amplitude. To simplify the molecular orientation calculations, only these two major elements are considered. With these approximations, eq 7 yields

$$\chi_{zzz} = \frac{\langle \cos^3\theta \rangle}{\langle \cos\theta \rangle}(\chi_{zzz} + 2\chi_{xzx}) + 2\frac{\langle \cos^2\theta \sin\theta \rangle}{\langle \sin\theta \rangle}(\chi_{zxx} - \chi_{xzx}) \quad (12)$$

where θ is the angle between the surface normal and the molecular z axis.[79] If one assumes a narrow distribution of the transition dipole about θ, eq 12 reduces to

$$\cos^2\theta = \frac{\chi_{zzz}}{\chi_{zzz} + \chi_{xxx}} \quad (13)$$

The angle θ corresponds to the apparent molecular tilt angle in the laboratory frame of reference. The ramifications of assuming a narrow distribution and a molecularly flat interface are addressed in section IV. Table 2 shows the two sets of $\chi^{(2)}$ elements and resulting tilt angles (θ) of 4ABP for four hydrophilic silica/liquid systems. The results show that 4ABP molecules adsorbed to strongly associating interfaces adopt a preferred average orientation closer to the surface normal relative to 4ABP adsorbed to weakly associating interfaces. Again, it is worth noting that both sets of $\chi^{(2)}$ elements for each system lead to calculated orientations that are internally consistent and indistinguishable within the limits of experimental uncertainty.

IV. Discussion

A. Interfacial Polarity and Solvent Structure. This section begins by considering the ways in which a hydrophilic surface can alter interfacial solvent polarity from bulk solution limits. Contributions to solvent polarity are generally divided into dipolar, dispersion, and induction effects.[44] For solutes showing bathochromic solvatochromism, these contributions add constructively and all terms help lower the observed transition energy from its gas-phase limit:

$$E_{soln} = E_{gas} + E_{solv} = E_{gas} + \sum_i E_i + = E_{gas} + E_{dipolar} + E_{dispersion} + E_{induced} \quad (14)$$

In eq 14, E_{gas} refers to a solute's gas-phase excitation energy, and E_{solv} corresponds to the change in excitation energy brought about by solvating the solute. The individual components of E_{solv}, E_i, are all negative and correspond to solvent−solute interactions that differentially lower the excited-state potential energy surface relative to the ground-state surface. When considering solute excitation, dipole−dipole interactions influence only the ground state of the system due to the solvent's inability to reorient around a new solute charge distribution during an electronic transition. Thus solvatochromic behavior of solute excitation depends only on the inertia-less modes of solvation.[44]

TABLE 3: Transition Energies (kJ/mol) and Differences between Interfacial and Bulk Solution Transition Energies for the Various Solvent Systems Studied[a]

solvent	E_{soln}	E_{surf}	ΔE	ΔE^*
cyclohexane	392.7	374.2	−18.5	0
CCl4	386.4	361.7	−24.7	−6.2
diisopropyl ether	374.2	365.0	9.2	+9.3
1-propanol	353.1	358.4	+5.3	(+23.8)
1-butanol	353.1	360.6	+7.5	(+25.9)
1-pentanol	353.1	359.5	+6.4	(+24.9)
1-hexanol	352.1	359.5	+7.4	(+25.8)
1-octanol	354.2	365.0	+10.8	(+29.3)
1-decanol	355.2	367.3	+12.1	(+30.6)
2-propanol	354.2	351.0	−3.2	(+15.3)
isobutyl alcohol	352.1	351.0	−1.1	(+17.4)

[a] ΔE^* refers to differences in surface-induced, nonadditive contributions to the interfacial transition energy and is derived from eq 15b using cyclohexane as a reference solvent.

In nonpolar solvents such as cyclohexane and carbon tetrachloride, the dipolar contributions to a solute's excitation energy are zero. Consequently, the observed 4ABP transition energies in cyclohexane (392.7 kJ/mol) and carbon tetrachloride (386.4 kJ/mol) reflect only dispersion and induction contributions (Table 3). Given a 4ABP gas-phase transition energy of 430.2 kJ/mol,[41] these contributions to E_{solv} for cyclohexane and carbon tetrachloride are −37.5 kJ/mol (cyclohexane) and −43.8 kJ/mol (CCl_4), respectively. Although both CCl_4 and cyclohexane have equivalent polarizabilities,[76] differences exist in the solvating properties between the two solvents due to the smaller size (and higher packing density) of CCl_4 relative to cyclohexane. Simple considerations based on molar densities show that a 4ABP solute has approximately 10−15% more nearest neighbors when dissolved in CCl_4 compared to cyclohexane. The higher density of nearest neighbors will lead to stronger dispersion and induction contributions to E_{solv} and a more pronounced red shift in the solute's excitation energy.[80]

If one considers 4ABP adsorbed to a hydrophilic solid/nonpolar solvent interface, the surface silanol groups will make a dipolar contribution to the overall solvation energy:

$$E_{surf} = E_{soln} + E_{SiOH} + E^* \quad (15a)$$

$$\Delta E = E_{surf} - E_{soln} = E_{SiOH} + E^* \quad (15b)$$

where E_{soln} is defined in eq 14, E_{SiOH} represents substrate−solute hydrogen bonding interactions, and E^* describes any additional contributions to the interfacial solvation energy arising

from effects such as partial desolvation or substrate-enhanced, interfacial solvent density. E_{SiOH} and E^* cannot be measured independently. However, differential effects can be assessed if E_{SiOH} is the same for different solid/liquid systems. This assumption should be valid for weakly associating systems (cyclohexane, CCl_4, isopropyl ether) but may not accurately describe strongly associating solid/liquid interfaces. Table 3 reports differences in E^* (ΔE^*) of different solid/liquid systems using ΔE of different solid/liquid systems and selecting cyclohexane as the reference solvent ($\Delta E^* = \Delta(\Delta E)$).

ΔE values for the cyclohexane and CCl_4 systems are -18.5 and -24.7 kJ/mol, respectively. Within experimental error, the change in solvation energy observed in the cyclohexane system corresponds to the contribution made by a single hydrogen bond. Choosing cyclohexane as a reference, ΔE^* for the CCl_4 system is negative (-6.2 kJ/mol), meaning that in addition to solute/substrate hydrogen bonding, the surface enhances local interfacial polarity relative to cyclohexane through some other mechanism. In contrast, ΔE^* for isopropyl ether is positive ($+9.3$ kJ/mol) despite the fact that isopropyl ether is more polar than either cyclohexane or CCl_4. The positive ΔE^* reflects a smaller surface-induced effect on interfacial polarity relative to the cyclohexane reference system.

The most striking conclusion from the cyclohexane, CCl_4, and isopropyl ether systems is that solvent structure plays an important role in determining interfacial solvent polarity. In all three systems, the substrate is the same, the solute is the same, and solvents are nonpolar (or weakly polar) with similar polarizabilities. The most significant difference is solvent shape. Both theory and simulation have shown that rigid surfaces create long-range order in an adjacent solvent and this surface-induced structure can extend for multiple solvent diameters.[19−22] The extent of surface-enhanced solvent density should depend sensitively on the balance of solvent−solvent and solvent−substrate forces, as well as the shape of the solvent molecules themselves.[81−83] For nonpolar solvents calculations suggest that solvent density can be up to 5 times higher than for bulk solution within the first several solvent layers.[81−83,19−22] Enhanced solvent density will increase a solvent's dispersion contributions to solute solvation, lowering the solute transition energy and creating a higher effective interfacial polarity. Per unit volume in bulk solution, CCl_4 packs ∼10% more efficiently than cyclohexane; isopropyl ether packs ∼20% less efficiently than cyclohexane. It is worth noting that experimental observations do not correlate with a solvent's isothermal compressibility, κ_T. Cyclohexane is 6% more compressible than CCl_4,[76] meaning that if κ_T were responsible for enhanced solvent density against a rigid wall, E^* for the silica/cyclohexane system should be more negative than for the silica/CCl_4 system.

The ΔE values for the *n*-alcohol/hydrophilic substrate systems range from $+15.3$ kJ/mol (1-propanol) to $+30.6$ kJ/mol (1-decanol). The positive sign corresponds to diminished solvent polarity at the liquid/solid interface relative to bulk solution. In light of the strongly associating nature of the solvent/substrate systems, the general trend is not surprising. Solvent/substrate hydrogen bonding will reduce the ability of the surface to impact directly the dipole interactions experienced by interfacial solute species. Furthermore, surface-induced changes in long-range solvent structure will inhibit solvent dipolar contributions to the solute's interfacial solvation energy. In the limiting case where all surface dipoles are hydrogen-bonded to *n*-alcohol solvent partners, the E_{SiOH} makes no contribution to ΔE in eq 15 and ΔE simply reflects E^* (not ΔE^*), the surface-mediated solvation term.

The positive sign of E^* in the strongly associating systems could be interpreted in one of two ways. If surface-enhanced solvent density leads to increased interfacial polarity ($\Delta E^* < 0$), then a positive E^* may reflect diminished solvent density at the solid/liquid boundary. Recent studies suggest that this situation arises at boundaries between a hydrophobic substrate and a protic solvent.[37] However, this explanation seems unlikely for the strongly associating systems considered here. A tightly packed monolayer of linear alcohol species would actually have local densities similar to those of bulk solution limits. A more likely explanation is that the surface-induced ordering of the *n*-alcohol solvent species reduces the dipolar contributions that appear in eq 14 (E_{dipole}) and eq 15 (E_{SiOH}), thereby reducing the effective solvent polarity and increasing the interfacial solute's excitation energy (leading to the observed blue shift).

Similar arguments are not applicable for the branched alcohol systems simply because solvent structure prevents formation of tightly packed interfacial monolayers, and unscreened surface dipoles can contribute to E_{SiOH}. Geometric considerations show that a close-packed monolayer of 2-propanol molecules at a hydrophilic silica surface leaves ∼ 2/3 of all surface dipoles unscreened and able to interact with adsorbed 4ABP solutes. Thus E_{SiOH} can contribute to ΔE and lower 4ABP's transition energy relative to bulk solution. The effect is not large compared to bulk solution (-3.1 kJ/mol for 2-propanol and only -1.0 kJ/mol for isobutanol) but the differences are significant when compared to results from the linear isomer systems at the same polar surface. Comparing both the linear and branched propanol and butanol systems, the change in ΔE is ∼-9 kJ/mol with the branched alcohol creating a more polar interfacial environment relative to the linear isomer.

B. Solvent Control of Solute Orientation at Hydrophilic Solid/Liquid Boundaries. Results from experiments examining solute orientation at weakly and strongly associating solid/liquid interfaces support the models developed to explain the origins of interfacial solvent polarity. Data in Figure 12 were used to calculate tilt angles of 46−49° and 38−39° for weakly (cyclohexane) and strongly associating (1-butanol) interfaces, respectively. If these results represent a narrow distribution of the transition moment's orientation relative to the surface normal, then the 4ABP solutes adsorbed to the weakly associating solid/liquid interfaces experience greater tilt than those solutes adsorbed to the strongly associating boundaries.

Such an interpretation assumes that the surface is molecularly flat and that the local tilt angle (in the molecular frame of reference) represents the apparent tilt angle (in the laboratory frame of reference). However, the optically flat silica prisms used in these experiments are not atomically flat over molecular length scales. Repeated atomic force measurements show a rms roughness of less than 1 nm over randomly selected 4-μm^2 areas on the prism face. Rowlen and co-workers have shown how both finite orientation distributions and local, microscopic surface topography can influence macroscopic measurements of molecular orientation.[79] Both broad distributions and rough surfaces randomize the angular distribution of solutes about the macroscopic surface normal. In the limit of very broad distributions (fwhm ≥ 30°) and/or very rough surfaces, apparent angular orientations as determined by polarization-dependent second harmonic measurements converge to a "magic angle" of 39°.[84]

In the systems presented here, the substrates and solutes *are always the same*. Thus, contributions from surface roughness *and* distributions in solute orientation should contribute equivalently to all systems studied. Nevertheless, polarization-dependent measurements of second harmonic intensity result in

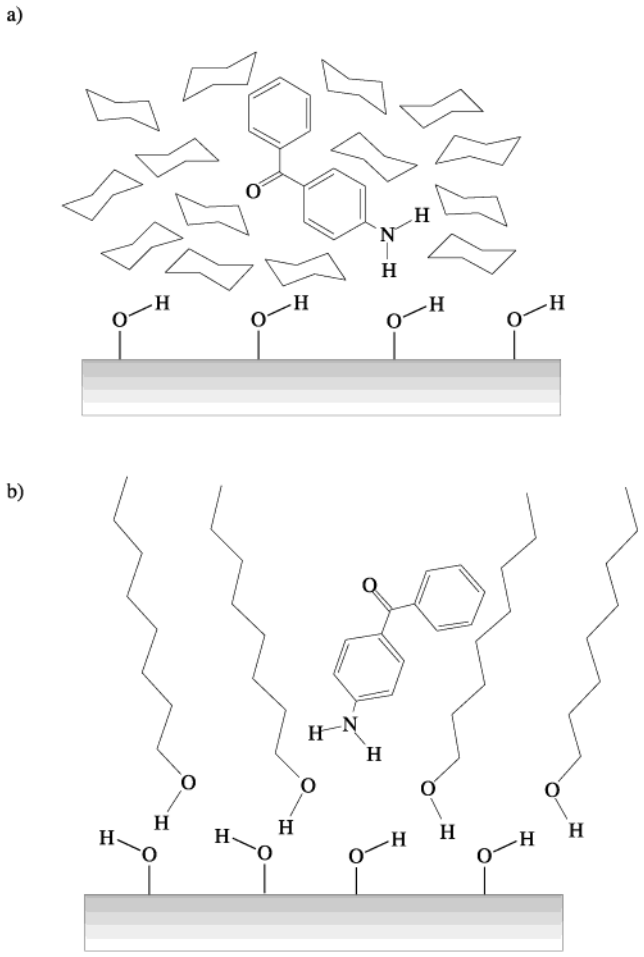

Figure 13. Qualitative diagram illustrating how surface dipoles can interact with adsorbed solutes in weakly associating systems but not in strongly associating systems. Orientation data indicate that 4ABP solutes adsorbed from nonpolar solvents are positioned with their transition moment aligned further away from the laboratory-fixed surface normal. Conversely, 4ABP adsorbed to strongly associating silica/*n*-alcohol interfaces adopt a more upright orientation.

different apparent molecular orientations depending on *the identity of the solvent*. Of the two types of systems examined—strongly and weakly associating—the weakly associating interface leads to larger 4ABP tilt angles (48°) than the strongly associating interface (38°). Based on topographical considerations, interfacial solutes in the strongly associating system may sample a "roughened" interface—the measured orientation matches the 39° magic angle—while in the weakly associating system, solutes would appear to adsorb to a more microscopically flat surface. Solute−substrate hydrogen bonding in the weakly associating systems will reduce the mobility of the 4ABP solutes and keep the solutes constrained in a more uniform angle distribution relative to the local surface structure. Furthermore, interactions between adjacent surface dipoles and the rest of the solute, especially the carbonyl, will tend to "pull" the solute closer to the surface (Figure 13). Given the measured rms roughness of the silica surfaces used in these experiments, an observed, apparent tilt angle of 46−49° does not deviate significantly from the predicted local tilt angle of ∼52−56° assuming a reasonably narrow orientational distribution of adsorbed solutes.[19]

The second variable that can affect the apparent orientation of solutes as calculated from polarization-dependent SH measurements is a spread in the orientation distribution. Results presented in Table 2 resulted from assuming a narrow orientation distribution of adsorbed solute species. Such an assumption is not unreasonable in the weakly associating systems given the opportunities for strong substrate/solute interactions. Orienation measurements of pyridinium dyes similarly hydrogen bonded to a silica substrate led to a measured orientation distribution of 8°.[79] Significantly broader distributions have been observed only for systems having a much higher degree of conformational flexibility. Solute orientation disitributions may be broader in the strongly associating systems studied here, due to solvent inhibited solute−substrate interactions. However, given the "magic-angle" results of Simpson and Rowlen, measurements of solute orientations in this work could accommodate distribution widths in excess of 20° without changing the underlying interpretation presented here.[79]

The smaller tilt angle of 38° observed in the strongly associating systems suggests that the 4ABP solutes adopt a more perpendicular or upright orientation at the interface. Given the roughness of the optical silica substrate, an apparent tilt angle of 38° actually corresponds to a slightly more erect local orientation ($\theta \sim 32-34°$).[79] If the solvent forms strong H-bonds with the substrate and a corresponding nonpolar region of well-ordered alkyl chains, interfacial solute species might be expected to align themselves along the direction defined by the alcohol chain axes. This picture is consistent with the interfacial solvent polarity data that imply little direct interaction between the solute and the hydrophilic substrate. Grazing angle X-ray experiments as well as molecular dynamics simulations have shown that long-chain, neutral amphiphiles adopt tilt angles of 0−33°, depending on amphiphilic surface density.[85,86] At surface concentrations of 5/nm^2 (to match the density of silanol groups on the hydrophilic substrate), the predicated tilt angle between the long axis of the alkyl chain and the surface normal is 20°.[85] Surface roughening may very well broaden and shift this distribution to apparent tilt angles of 30° or more.[19]

V. Conclusions

Resonance-enhanced SHG spectra of 4ABP adsorbed to different solid/liquid boundaries show that interfacial solvent polarity is controlled by a number of factors. Substrate−solvent interactions are the dominant influence. In systems where nonpolar solvents are only weakly attracted to hydrophilic silica surfaces, surface dipoles can interact strongly with adsorbed solutes, creating more polar environments than are found in bulk solutions. This effect was observed for silica/cyclohexane and silica/CCl_4 systems as well as the silica/diisopropyl ether interface. However, when the substrate and solvent couple through hydrogen bonding, interfacial dielectric properties depend quite sensitively on the solvent's molecular structure. Spectra of 4ABP adsorbed to silica/*n*-alcohol boundaries show that the solute samples an environment that reflects neither the properties of the substrate nor the properties of the solvent. Such nonadditive interfacial behavior can result from formation of oriented *n*-alcohol monolayers at the hydrophilic silica surface. Extensive hydrogen bonding between the substrate and solvent not only prevents surface−solute interactions but also inhibits full solvation of the solute by the surrounding solvent. In the limit that the *n*-alcohol alkyl chains form well-ordered regions extending away from the silica substrate, adsorbed 4ABP solutes will experience a local, interfacial environment that is significantly less polar than bulk solution. Spectra show that the interfacial region becomes increasingly nonpolar as *n*-alcohol chain length increases. If, however, the protic solvent cannot form such a well-ordered, long-range structure, surface dipoles can go unscreened and again interact with interfacial solutes.

This situation arises when 4ABP adsorbs to a hydrophilic substrate from 2-propanol and, to a lesser extent, from isobutyl alcohol. These results are significant because they demonstrate the important role that solvent structure plays in determining the effective interfacial polarity experienced by adsorbed solutes. Solvents having similar bulk dielectric properties create *qualitatively* different environments at the solid/liquid interface.

A secondary effect of solvent structure on interfacial polarity appears to be related to solvent size and packing ability. Solvatochromic results show the interfacial region between a hydrophilic silica substrate and CCl_4 is disproportionately more polar than the equivalent hydrophilic silica/cyclohexane boundary. Given the similarities in dielectric properties between CCl_4 and cyclohexane as well as the equivalent solute−substrate interactions in the two systems, the enhanced polarity across the silica/CCl_4 interface seems surprising. We propose that differences between interfacial CCl_4 and cyclohexane are due to the former's ability to pack efficiently next to a rigid, solid boundary, thereby increasing local solvent density over bulk solution limits. This idea is consistent with simple density arguments as well as statistical models describing distribution functions of hard spheres against rigid walls. Enhanced interfacial density of the spherical CCl_4 solvent will lead to amplified solvent−solute dispersion interactions and a correspondingly more polar environment than in bulk solution. Cyclohexane simply cannot pack as efficiently and thus cannot create the same environment at the hydrophilic silica surface.

Measurements of solute orientation at different hydrophilic solid/liquid interfaces reinforce the idea that solvent−solute interactions play a primary role in controlling interfacial solvation. Solid/liquid systems that associate only weakly are amenable to strong substrate−solute interactions. These strong interactions manifest themselves through a large (and negative) ΔG_{ads} as well as a solute orientation that is deflected significantly away from surface normal. Deflections of ∼50° were observed for the weakly associating systems of hydrophilic silica/cyclohexane and hydrophilic silica/hexadecane. For strongly associating systems, hydrogen bonding between the substrate and solvent inhibit dipolar solvent−solute *and* solute−substrate interactions, and the solute adopts a more upright orientation with its major axis more closely aligned along the surface normal. Apparent tilt angles of ∼38° were observed for the hydrophilic silica/1-butanol and 1-octanol systems. Influences of surface roughness and broad orientation distributions are unlikely to alter these interpretations, given that the surfaces and solutes were identical in all of the systems studied.

Acknowledgment. We thank Professor Jack Tossell for carrying out ab initio structure calculations for the ground and excited states of 4ABP and the Sita research group for AFM measurements of the quartz substrates. Professor John Weeks is also thanked for illuminating conversations. This work was supported by the National Science Foundation through the CAREER program (CHE0094246) and through generous donations of equipment from Clark-MXR, Inc. M.C. gratefully acknowledges support from the Rollinson Fellowship Program and the Howard Hughes Medical Institute.

References and Notes

(1) Mills, A. L.; Herman, J. S.; Hornberger, G. M.; Dejesus, T. H. *Appl. Environ. Microbiol.* **1994**, *60*, 3300−3306.
(2) Naidja, A.; Huang, P. M.; Bollag, J. M. *J. Environ. Qual.* **2000**, *29*, 677−691.
(3) Hartgerink, J. D.; Beniash, E.; Stupp, S. I. *Science* **2001**, *294*, 1684−1688.
(4) Murphy, W. L.; Mooney, D. J. *J. Am. Chem. Soc.* **2002**, *124*, 1910−1917.
(5) Addadi, L.; Weiner, S. *Nature* **2001**, *411*, 753−755.
(6) *Chemical Modified Surfaces in Catalysis and Electrocatalysis*; Miller, J. S., Ed.; American Chemical Society: Washington, DC, 1982; Vol. 192, p 301.
(7) Stefanovich, E. V.; Truong, T. N. *J. Chem. Phys.* **1997**, *106*, 7700−7705.
(8) *Dynamic Process on Solid Surfaces*; Tamaru, K., Ed.; Plenum Press: New York, 1993; p 357.
(9) *Supported Catalysts and Their Applications*; Sherrington, D. C., Ktbett, A. P., Eds.; Royal Society of Chemistry: Cambridge, 2001; Vol. 192, p 270.
(10) Liu, X. Y.; Bennema, P. *J. Chem. Phys.* **1993**, *98*, 5863−5872.
(11) Benjamin, I. *Chem. Rev.* **1996**, *96*, 1449−1475.
(12) Chipot, C.; Wilson, M. A.; Pohorille, A. *J. Phys. Chem. B* **1997**, *101*, 782−791.
(13) Dang, L. X. *J. Phys. Chem. B* **2001**, *105*, 804−809.
(14) Yeh, I. C.; Berkowitz, M. L. *J. Chem. Phys.* **1999**, *110*, 7935−7942.
(15) Tikhonov, A. M.; Mitrinovic, D. M.; Li, M.; Huang, Z.; Schlossman, M. L. *J. Phys. Chem. B* **2000**, *104*, 6336−6339.
(16) Yu, C. J.; Evmenenko, G.; Richhter, A. G.; Datta, A.; Kmetko, J.; Dutta, P. *Appl. Surf. Sci.* **2001**, *182*, 231−235.
(17) Eisenthal, K. B. *Chem. Rev.* **1996**, *96*, 1343−1360.
(18) Corn, R. M.; Higgins, D. A. *Chem. Rev.* **1994**, *94*, 107−125.
(19) Snook, I. K.; Henderson, D. *J. Chem. Phys.* **1978**, *68*, 2134−2139.
(20) Segura, C. J.; Chapman, W. G. *Mol. Phys.* **1995**, *86*, 415−442.
(21) Götzelmann, B.; Haase, H.; Dietrich, S. *Phys. Rev. E* **1996**, *53*, 3456−3467.
(22) Patra, C. N. *J. Chem. Phys.* **1999**, *11*, 6573−6578.
(23) Wang, H.; Borguet, E.; Eisenthal, K. B. *J. Phys. Chem. A* **1997**, *101*, 713−718.
(24) Wang, H.; Borguet, E.; Eisenthal, K. B. *J. Phys. Chem. B* **1998**, *102*, 4927−4932.
(25) Michael, D.; Benjamin, I. *J. Phys. Chem.* **1995**, *99*, 16810−16813.
(26) Michael, D.; Benjamin, I. *J. Chem. Phys.* **1997**, *107*, 5684−5693.
(27) Michael, D.; Benjamin, I. *J. Phys. Chem. B* **1998**, *102*, 5145−5151.
(28) Squitieri, E.; Benjamin, I. *J. Phys. Chem. B* **2001**, *105*, 6412−6419.
(29) Ishizaka, S.; Habuchi, S.; Kim, H. B.; Kitamura, N. *Anal. Chem.* **1999**, *71*, 3382−3389.
(30) Ishizaka, S.; Kim, H. B.; Kitamura, N. *Anal. Chem.* **2001**, *73*, 2421−2428.
(31) Croxton, C. A. *Statistical Mechanics of the Liquid Surface*; J. Wiley: New York, 1980.
(32) Bublitz, G. U.; Boxer, S. G. *J. Am. Chem. Soc.* **1998**, *120*, 3988−3922.
(33) Adams, J. E. *J. Phys. Chem. B* **1998**, *102*, 7455−7461.
(34) Yanigamchi, M.; Tamai, N.; Masuhara, H. *Chem. Phys. Lett.* **1992**, *200*, 469−474.
(35) Meech, S. R.; Yoshihara, K. *Chem. Phys. Lett.* **1990**, *174*, 423−427.
(36) Meech, S. R.; Yoshihara, K. *J. Chem. Phys.* **1990**, *94*, 4913−4920.
(37) Zhang, X.; Esenturk, O.; Walker, R. A. *J. Am. Chem. Soc.* **2001**, *123*, 10 768−10 769.
(38) Zhang, X.; Walker, R. A. *Langmuir* **2001**, *17*, 4486-4489.
(39) Onsager, L. *J. Am. Chem. Soc.* **1936**, *58*, 1486-1493.
(40) Kirkwood, J. G. *J. Chem. Phys.* **1939**, *7*, 911−919.
(41) Takahashi, K.; Abe, K.; Sawamura, S.; Jonah, C. D. *Chem. Phys. Lett.* **1998**, *282*, 361−368.
(42) Suppan, P.; Ghoneim, N. *Solvatochromism*; Royal Society of Chemistry: Cambridge, U.K., 1997.
(43) Suppan, P. *J. Photochem. Photobiol. A: Chem.* **1990**, *50*, 293−330.
(44) Matyushov, D. V.; Schmid, R.; Ladanyi, B. M. *J. Phys. Chem. B* **1997**, *101*, 1035−1050.
(45) Böttcher, C. J. F.; Bordewijk, P. *Theory of Electric Polarization*, 2 ed.; Elsevier Scientific Publishing Company: Amsterdam, Oxford, New York, 1978; Vol. 2.
(46) McRae, E. G. *J. Phys. Chem.* **1957**, *61*, 562−572.
(47) Laurence, C.; Nicolet, P.; Dalati, M. T.; Abboud, J. M.; Notario, R. *J. Chem. Phys.* **1994**, *98*, 5807−5816.
(48) Perera, J. M.; Stevens, G. W.; Grieser, F. *Colloids Surf. A* **1995**, *95*, 185−192.
(49) Brot, C. *Mol. Phys.* **1982**, *45*, 543−552.
(50) Cossi, M.; Rega, N.; Scalmani, G.; Barone, V. *J. Chem. Phys.* **2001**, *114*, 5691−5701.
(51) Wong, M. W.; Frisch, M. J.; Wiberg, K. B. *J. Am. Chem. Soc.* **1991**, *113*, 4776−4782.
(52) Singh, A. K.; Bhasikuttan, A. C.; Palit, D., K.; Mittal, J. P. *J. Phys. Chem.* **2000**, *104*, 7002−7009.

(53) Shen, Y. R. *The Principles of Nonlinear Optics*; John Wiley and Sons: New York, 1984.
(54) Dadap, J. I.; Heinz, T. F. Nonlinear optical spectroscopy of surfaces and interfaces. In *Encyclopedia of Chemical Physics and Physical Chemistry*; Moore, J. H., Spencer, N. D., Eds.; Institute of Physics Publishing: Philadelphia, 2001; Vol. 2, pp 1089−1127.
(55) Reichardt, C. *Chem. Rev.* **1994**, *94*, 2319−2358.
(56) Shen, Y. R. *Nature* **1989**, *337*, 519−525.
(57) Xu, Z.; Dong, Y. *Surf. Sci. Lett.* **2000**, *445*, L65-L70.
(58) Zimdars, D.; Dadap, J. I.; Eisenthal, K. B.; Heinz, T. F. *Chem. Phys. Lett.* **1999**, *301*, 112−120.
(59) Zimdars, D.; Dadap, J. I.; Eisenthal, K. B.; Heinz, T. F. *J. Phys. Chem. B* **1999**, *103*, 3425−3433.
(60) Dick, B.; Gierulski, A.; Marowsky, G.; Reider, G. A. *Appl. Phys. B* **1985**, *38*, 107−116.
(61) Miranda, P. B.; Pflumio, V.; Saijo, H.; Shen, Y. R. *J. Am. Chem. Soc.* **1998**, *120*, 12 092−12 099.
(62) Pople, J. A. *J. Chem. Soc., Faraday Trans.* **1953**, *49*, 1375−1385.
(63) Praiser, R.; Parr, R. G. *J. Chem. Phys.* **1953**, *21*, 466−471.
(64) Praiser, R.; Parr, R. G. *J. Chem. Phys.* **1953**, *21*, 767−776.
(65) Li, D.; Ratner, M. A.; Marks, T. J. *J. Am. Chem. Soc.* **1988**, *110*, 1707−1705.
(66) Dirk, C. W.; Twieg, R. J.; Wagnière, G. *J. Am. Chem. Soc.* **1986**, *108*, 5387−5395.
(67) Gee, M. L.; Healy, T. W.; White, L. R. *J. Colloid Interface Sci.* **1990**, *140*, 450−465.
(68) Ong, S.; Zhao, X.; Eisenthal, K. B. *Chem. Phys. Lett.* **1992**, *191*, 327−335.
(69) Wang, H.; Harris, J. M. *J. Phys. Chem.* **1995**, *99*, 16999−17009.
(70) Elking, M. D.; He, G.; Xu, Z. *J. Chem. Phys.* **1996**, *105*, 6565−6573.
(71) Simpson, G. J.; Westerbuhr, S. G.; Rowlen, K. L. *Anal. Chem.* **2000**, *72*, 887−898.
(72) Ekhoff, J. A.; Westerbuhr, S. G.; Rowlen, K. L. *Lamgmuir* **2001**, *17*, 7079−7084.
(73) Xu, Z.; Lu, W.; Bohn, P. W. *J. Phys. Chem.* **1995**, *99*, 7154−7159.
(74) Hiemenz, P. C.; Rajagopalan, R. *Principles of Colloid and Surface Chemistry*, 3 ed.; Marcel Dekker: New York, 1997.
(75) *Adsorption on Silica Surface*; Papirer, E., Ed.; New York, 2001; p 735.
(76) *CRC Handbook of Chemistry and Physics*, 72 ed.; Lide, D. R., Ed.; CRC Press: Boston, 1991.
(77) Stanners, C. D.; Du, Q.; Chin, R. P.; Cremer, P.; Somojai, G. A.; Shen, Y. R. *Chem. Phys. Lett.* **1995**, *232*, 407−413.
(78) Ocko, B. M.; Wu, X. Z.; Sirota, E. B.; Sinha, S. K.; Deutsch, M. *Phys. Rev. Lett.* **1994**, *72*, 242−245.
(79) Simpson, G. J.; Rowlen, K. L. *Acc. Chem. Res.* **2000**, *33*, 781−789.
(80) Ben-Amotz, D.; Omelyan, I. *J. Chem. Phys.* **2001**, *115*, 9401−9409.
(81) Kotelyanskii, M. J.; Hentschke, R. *Phys. Rev. E* **1994**, *49*, 911−913.
(82) Smith, P.; Lynden-Bell, R. M.; Earnshaw, J. C.; Smith, W. *Mol. Phys.* **1999**, *96*, 249−257.
(83) Smith, P.; Lynden-Bell, R. M.; Smith, W. *Mol. Phys.* **2000**, *98*, 255−260.
(84) Simpson, G. J.; Rowlen, K. L. *J. Am. Chem. Soc.* **1999**, *121*, 2635−2636.
(85) Karaborni, S.; Toxvaerd, S. *J. Chem. Phys.* **1992**, *97*, 5876−5883.
(86) Xia, T. K.; Landman, U. *Phys. Rev. B* **1993**, *48*, 11 313−11 316.